SANDIA REPORT

SAND2018-3068 Unlimited Release Printed March 2018

Measuring Balance Across Multiple Radar Receiver Channels

Armin W. Doerry and Douglas L. Bickel

Prepared by Sandia National Laboratories Albuquerque, New Mexico 87185 and Livermore, California 94550

Sandia National Laboratories is a multimission laboratory managed and operated by National Technology and Engineering Solutions of Sandia, LLC., a wholly owned subsidiary of Honeywell International, Inc., for the U.S. Department of Energy's National Nuclear Security Administration under contract DE-NA-0003525.

Approved for public release; further dissemination unlimited.



Issued by Sandia National Laboratories, operated for the United States Department of Energy by Sandia Corporation.

NOTICE: This report was prepared as an account of work sponsored by an agency of the United States Government. Neither the United States Government, nor any agency thereof, nor any of their employees, nor any of their contractors, subcontractors, or their employees, make any warranty, express or implied, or assume any legal liability or responsibility for the accuracy, completeness, or usefulness of any information, apparatus, product, or process disclosed, or represent that its use would not infringe privately owned rights. Reference herein to any specific commercial product, process, or service by trade name, trademark, manufacturer, or otherwise, does not necessarily constitute or imply its endorsement, recommendation, or favoring by the United States Government, any agency thereof, or any of their contractors or subcontractors. The views and opinions expressed herein do not necessarily state or reflect those of the United States Government, any agency thereof, or any of their contractors.

Printed in the United States of America. This report has been reproduced directly from the best available copy.

Available to DOE and DOE contractors from

U.S. Department of Energy Office of Scientific and Technical Information P.O. Box 62 Oak Ridge, TN 37831

Telephone: (865) 576-8401 Facsimile: (865) 576-5728

E-Mail: reports@adonis.osti.gov Online ordering: http://www.osti.gov/bridge

Available to the public from

U.S. Department of Commerce National Technical Information Service 5285 Port Royal Rd. Springfield, VA 22161

Telephone: (800) 553-6847 Facsimile: (703) 605-6900

E-Mail: <u>orders@ntis.fedworld.gov</u>

Online order: http://www.ntis.gov/help/ordermethods.asp?loc=7-4-0#online



SAND2018-3068 Unlimited Release Printed March 2018

Measuring Balance Across Multiple Radar Receiver Channels

Armin W. Doerry ISR Mission Engineering

Douglas L. Bickel ISR Analysis & Applications

Sandia National Laboratories PO Box 5800 Albuquerque, NM 87185-0519

Abstract

When radar receivers employ multiple channels, the general intent is for the receive channels to be as alike as possible, if not as ideal as possible. This is usually done via prudent hardware design, supplemented by system calibration. Towards this end, we require a quality metric for ascertaining the goodness of a radar channel, and the degree of match to sibling channels. We propose a relevant and useable metric to do just that.

Acknowledgements

This report was the result of an unfunded research and development activity.

Contents

Foreword			
		fication	
		r Contact Information	
1		oduction and Background	
2	Deta	ailed Discussion	
	2.1	Some Basic Definitions	9
	2.2	Ideal Channel	0
	2.3	Non-Ideal Channel	
	2.4	Channel Similarity Measure	
	2.4.		
	2.4.	2 Amplitude Difference	5
	2.4.		
	2.5	Channel Similarity Measure – Small Errors	6
	2.6	Matched Filter Analysis	7
	2.6.		
	2.6.	1	
	2.7	Comparing Channels to Ideal	20
	2.8	Comparing Channels to Each Other	
	2.9	Relationship to Coherence Measure	
	2.10	Ideal Nonlinear Channels	
	2.11	Secondary Issues	
	2.11		
	2.11		
	2.11		
	2.12	Frequency Sampling Issues	
3	Exa	mples of Imbalance Effects	
	3.1.		
	3.1.	8	
	3.1.		
	3.1.		
	3.1.		
	3.1.		
4		v Good is Good Enough?	
	4.1	Comparing Channels to Ideal	
	4.2	Comparing Channels to Each Other	
	4.3	Imbalance Mitigation Techniques	
5		clusions2	
Re	eference	es	
D	etributi	ion	10

Foreword

This report details the results of an academic study. It does not presently exemplify any modes, methodologies, or techniques employed by any operational system known to the authors.

Classification

The specific mathematics and algorithms presented herein do not bear any release restrictions or distribution limitations.

This report formalizes preexisting informal notes and other documentation on the subject matter herein.

Author Contact Information

Armin Doerry <u>awdoerr@sandia.gov</u> 505-845-8165 Douglas Bickel <u>dlbicke@sandia.gov</u> 505-845-9038

1 Introduction and Background

A simple radar system transmits from a single source, and receives with a single antenna, and further processes with simple algorithms a single echo signal characteristic. Such a receiver exhibits a single receiver channel. Additional information from a diversity of received signal characteristics often allows target discrimination with increased reliability, sensitivity, precision, and/or accuracy. Such systems will generally process two or more distinct signal characteristics, each with its own processing channel.

Examples of multi-channel radar receivers include:

- 1. Interferometric Synthetic Aperture Radar (IFSAR, InSAR)
- 2. Ground Moving Target Indicator (GMTI), or Dismount Moving Target Indicator (DMTI) radar, with sub-clutter visibility.
- 3. Tracking radars
- 4. Direction-finding modes
- 5. Polarimetric radars
- 6. Quadrature Demodulation channels

In all cases, the distinct radar channels seek to process specific inputs so that differences in the inputs can be analyzed and assessed. That is, the purpose of the different channels is to help assess the different "inputs," with differences in the channels themselves made irrelevant to the final comparison. We want our final answer to be about the input signals, and not confused by variations or perturbations of the signal path within the radar. This necessitates eliminating differences in the processing channels, or at the very least identifying and understanding them.

While we desire that multiple channels all exhibit ideal characteristics with respect to processing or in the transmission of signals, alas we must allow that real systems will not be perfect. However, with multiple channels we are often more interested in "differences" of their signals, implying that "relative" channel performance properties may have different requirements, even stricter requirements, than the individual channels with respect to ideal. That is, channel "balance" requirements are often different, and perhaps more strict, than their individual allowable non-idealness.

The authors have repeatedly observed that well-calibrated and balanced channels often make the difference between success and failure of a radar application/mission. Clearly, to fix something, you first must be able to measure it. Otherwise you can't know that it even needs fixing, let alone that it was ever fixed thereafter. Consequently, in this report we examine channel balance measures, and specific balance metrics.

Nature abounds in multi-channel sensors, to facilitate capabilities beyond single-channel systems. Symmetric and balanced sensor arrays for sound and sight are the norm.



Figure 1. Stereoscopic image pair of hotel walkway. (Hold page about 8 to 10 inches in front of face so that each eye views its own frame.)

2 Detailed Discussion

2.1 Some Basic Definitions

To set up the following discussion, we begin by defining a generic signal

$$x(t) = \text{continuous function of time } t.$$
 (1)

As we will be interested in the Fourier Transform of functions, we accordingly define

$$X(f) = \int_{-\infty}^{\infty} x(t)e^{-j2\pi ft}dt = \text{forward transform, and}$$

$$x(t) = \int_{-\infty}^{\infty} X(f)e^{j2\pi ft}df = \text{inverse transform,}$$
(2)

where the Fourier Transform is in terms of frequency f. We may use shorthand to identify the transform pair as

$$x(t) \Leftrightarrow X(f)$$
. (3)

We shall consider applying such a signal to a receiver channel, which we identify as a Linear Time-Invariant (LTI) filter function, where the channel and its transform are identified as

$$h(t) \Leftrightarrow H(f).$$
 (4)

Conventionally, we identify

$$h(t)$$
 = channel/filter "impulse response" (IPR), and $H(f)$ = channel/filter "transfer function," or "frequency response." (5)

The output of applying this channel/filter to the input signal is calculated as

$$y(t) = h(t) * x(t) = \int_{-\infty}^{\infty} h(t - \tau)x(\tau)d\tau, \text{ and}$$

$$Y(f) = H(f)X(f).$$
 (6)

Here, the symbol "*" denotes convolution.

Of course, the output functions are related as

$$y(t) \Leftrightarrow Y(f)$$
. (7)

We note that for this report, a signal transmission channel can be characterized as essentially a filter function. We will often use these terms interchangeably.

2.2 Ideal Channel

For our purposes, we begin with the concept of a distortionless channel/filter, with attendant form

$$h_{distortionless}(t) = C_{ideal}\delta(t - T_{ideal}), \tag{8}$$

where

$$C_{ideal}$$
 = constant gain, and T_{ideal} = constant delay. (9)

The spectrum of this distortionless channel is calculated as

$$H_{distortionless}(f) = C_{ideal}e^{-j2\pi T_{ideal}f}.$$
 (10)

Note that this has infinite frequency-extent of its frequency response; infinite bandwidth. For our purposes, an ideal channel is one that is distortionless over some limited band of interest

$$H_{ideal}(f) = H_{distortionless}(f) \operatorname{rect}\left(\frac{f - f_{ideal}}{B_{ideal}}\right), \tag{11}$$

where the new quantities are

 f_{ideal} = ideal channel center frequency,

 B_{ideal} = ideal channel bandwidth, and

$$\operatorname{rect}(\zeta) = \begin{cases} 1 & |\zeta| < 1/2 \\ 1/2 & |\zeta| = 1/2 \\ 0 & else \end{cases}$$
 (12)

This, of course, allows us to infer that

$$h_{ideal}(t) = h_{distortionless}(t) * \left(B_{ideal}\operatorname{sinc}(B_{ideal}t)e^{j2\pi f_{ideal}t}\right), \tag{13}$$

where we define and relate the functions

$$\operatorname{sinc}(\zeta) = \frac{\sin(\pi \zeta)}{\pi \zeta}$$
, and $\operatorname{rect}(f) \Leftrightarrow \operatorname{sinc}(t)$. (14)

We may explicitly write the ideal channel functions as

$$h_{ideal}(t) = C_{ideal}B_{ideal}\operatorname{sinc}\left(B_{ideal}(t - T_{ideal})\right)e^{j2\pi f_{ideal}(t - T_{ideal})}, \text{ and}$$

$$H_{ideal}(f) = C_{ideal}e^{-j2\pi T_{ideal}f_{ideal}}e^{-j2\pi T_{ideal}(f - f_{ideal})}\operatorname{rect}\left(\frac{f - f_{ideal}}{B_{ideal}}\right). \tag{15}$$

In particular, we note that the ideal transfer function is constant-amplitude, and linear phase (with frequency). This allows us to more generally write the transfer function as

$$H_{ideal}(f) = A_{ideal}(f)e^{j\Phi_{ideal}(f)}\operatorname{rect}\left(\frac{f - f_{ideal}}{B_{ideal}}\right),\tag{16}$$

where for the ideal channel

$$A_{ideal}(f) = C_{ideal} = \text{constant amplitude across the passband, and}$$

$$\Phi_{ideal}(f) = -2\pi T_{ideal}f = \text{linear phase across the passband.}$$
(17)

2.3 Non-Ideal Channel

The previous development has set us up to define a more general channel transfer function, or set of channel transfer functions as

$$H_k(f) = A_k(f)e^{j\Phi_k(f)}\operatorname{rect}\left(\frac{f - f_k}{B_k}\right),\tag{18}$$

where the constituent parameters and functions are

k = index denoting a particular channel,

 $A_k(f)$ = positive real-valued amplitude function across the passband for channel k,

 $\Phi_k(f)$ = real-valued phase function across the passband for channel k,

 f_k = nominal center reference frequency for the passband for channel k,

 B_k = nominal bandwidth of the passband for channel k, and

 $T_k(f)$ = nominal group delay of a signal through the channel for channel k. (19)

For completeness, we also identify the corresponding channel impulse response with

$$h_k(t) \Leftrightarrow H_k(f)$$
. (20)

As a practical matter, for transmission channels, we normally expect the amplitude function $A_k(f)$ to be relatively smoothly varying with frequency f across the passband. We furthermore normally expect that the unwrapped phase function $\Phi_k(f)$ will also be a relatively smoothly-varying function of frequency f, and with a typically strong linear component.

The group delay parameter T_k is not overtly present in the channel function as written in Eq. (18), but may be considered related to the linear phase component in $\Phi_k(f)$; in particular its frequency slope. It will become important later in this report. For now, we simply identify it as the group delay of the channel and generally a function of frequency, that is

$$T_k(f) = -\left(\frac{1}{2\pi}\right)\frac{d}{df}\Phi_k(f). \tag{21}$$

Although mentioned above, we have made the tacit assumption that the phase is "unwrapped," that is, does not contain any 2π jumps. If we need a single number and not a varying function of frequency, then we might calculate the group delay at band center, or perhaps some average value over the band of interest. This might also be related to the location of the peak of the impulse response.

The ideal situation for us is that all channels in a set are alike, and in fact identical to the ideal channel previously discussed. That is, we desire

$$H_k(f) = H_{ideal}(f)$$
, for each and every channel k . (22)

Failing being ideal, we would then desire that all channels at least be alike. That is, we then desire

$$H_k(f) = H_l(f)$$
, for each and every non-ideal channel pair k and l . (23)

The intent is that any differences in channel outputs be attributed to differences in their inputs, and not due to differences in the channels themselves. Sadly, neither of these situations can be reasonably expected with real hardware. Consequently, we need a measure of similarity between channels, including the ideal channel, to gauge non-ideal characteristics.

Finally, we will proceed with the assumption that any measurements of channel properties are high-fidelity, collected in a manner so as to be minimally impacted by measurement noise, or other measurement distortion.

2.4 Channel Similarity Measure

The conventional technique of measuring channel/filter characteristics is with a network analyzer, which measures gain and phase shift over a set of frequencies. That is, it measures the transfer function over a set of sample frequencies. Using 2-port Scattering-parameters (S-parameters), this is the S₂₁, or forward voltage gain, measure. Consequently, we will presume as input to any similarity measure the channel transfer function, and will calculate other measures from these.

We root our similarity measure in the concept of Euclidean distance, or L^2 norm. This is tractable because energy/power is proportional to the square of signal voltage, so minimizing the squared-error is minimizing the energy/power in the error. Accordingly, we define the error between two channels as

$$E_{k,l}(f) = H_k(f) - H_l(f) = \text{channel difference/error},$$
 (24)

and from this, we identify

$$\left|E_{k,l}(f)\right|^2 = \text{squared-error.}$$
 (25)

This squared-error is really an Energy Spectral Density (ESD), and may be expanded to

$$|E_{k,l}(f)|^2 = |H_k(f)|^2 + |H_l(f)|^2 - 2\operatorname{Re}\{H_k(f)\overline{H}_l(f)\},$$
 (26)

where we define the complex conjugate as

$$\overline{H}_l(f) = \text{complex conjugate of } H_l(f).$$
 (27)

So, we observe that the error ESD, $\left|E_{k,l}(f)\right|^2$, is really the difference between the sum of the individual channel ESDs, $\left|H_k(f)\right|^2 + \left|H_l(f)\right|^2$, and the product $2\operatorname{Re}\left\{H_k(f)\overline{H}_l(f)\right\}$. As such, we may normalize the error ESD by defining

$$\eta(f) = \frac{\left|E_{k,l}(f)\right|^2}{\left|H_k(f)\right|^2 + \left|H_l(f)\right|^2} = \text{normalized error measure.}$$
 (28)

We are, of course, assuming no mutual nulls in the channel ESDs, at least over the frequency spans of interest. In fact, there is an implicit limitation on the frequency span such that

$$\operatorname{rect}\left(\frac{f - f_k}{B_k}\right) = \operatorname{rect}\left(\frac{f - f_l}{B_l}\right),\tag{29}$$

and subsequent measures are also limited to this frequency span. Substantially different bandwidths have a number of implications, most of them not very nice. An example is that the same noise ESD will yield different noise energies. In any case, we assume that Eq. (29) holds true, and accept the favor that this gives us. We proceed and calculate the normalized error in Eq. (28) might be expanded and transmogrified to

$$\eta(f) = 1 - \left[\frac{\left(\sqrt{|H_{k}(f)|^{2} |H_{l}(f)|^{2}}\right)}{\left(\frac{|H_{k}(f)|^{2} + |H_{l}(f)|^{2}}{2}\right)} \right] \operatorname{Re} \left\{ \frac{H_{k}(f) \overline{H}_{l}(f)}{\sqrt{|H_{k}(f)|^{2} \sqrt{|H_{l}(f)|^{2}}}} \right\}.$$
(30)

Relating this to specific amplitude and phase components, and limiting our attention over a common passband of relevant frequencies, allows us to identify

$$\eta(f) = 1 - \left[\frac{\left(\sqrt{A_k^2(f) A_l^2(f)} \right)}{\left(\frac{A_k^2(f) + A_l^2(f)}{2} \right)} \right] \operatorname{Re} \left\{ e^{j(\Phi_k(f) - \Phi_l(f))} \right\}.$$
(31)

We rewrite this as, and define a Figure of Merit (FOM) as

$$FOM(f) = 1 - \eta(f) = \left[\frac{\left(\sqrt{A_k^2(f)A_l^2(f)}\right)}{\left(\frac{A_k^2(f) + A_l^2(f)}{2}\right)} \right] \cos\left(\Phi_k(f) - \Phi_l(f)\right). \tag{32}$$

We have retained this FOM as a function of frequency. The FOM is real-valued for all relevant frequencies. If both channels match each other perfectly, the normalized error is zero, and the FOM is unity for all relevant frequencies. We also note that the FOM is a product of contributions from

- 1. A function of the phase differences, and
- 2. A function of the individual amplitude terms (the individual ESD).

We examine these individually.

2.4.1 Phase Difference

One component of our FOM is due to phase differences. We define this component as

$$FOM_{phase}(f) = \cos(\Phi_k(f) - \Phi_l(f)). \tag{33}$$

Clearly, this FOM component is between -1 and +1, with +1 only possible if the phases are equal.

2.4.2 Amplitude Difference

The other component of our FOM is due to amplitude differences. We define this component as

$$FOM_{amplitude}(f) = \frac{\sqrt{A_k^2(f)A_l^2(f)}}{\left(\frac{A_k^2(f) + A_l^2(f)}{2}\right)}.$$
(34)

We observe that the numerator is a geometric mean of the ESDs, and the denominator is the arithmetic mean of the ESDs, both at a specified frequency. In general, by the theorem of inequality of arithmetic and geometric means, these are related by

$$\sqrt{A_k^2(f)A_l^2(f)} \le \left(\frac{A_k^2(f) + A_l^2(f)}{2}\right),\tag{35}$$

with equality holding only when $A_k^2(f) = A_l^2(f)$, and since amplitude functions are by definition positive, only when $A_k(f) = A_l(f)$. Consequently

$$0 \le FOM_{amplitude}(f) \le 1, \tag{36}$$

with unity value inferring that $A_k(f) = A_l(f)$.

2.4.3 Comments

We have above developed figures of merit for how well two channels match each other. Clearly, we can calculate frequency dependent functions for how well two amplitude-functions match each other, and how well two phase-functions match each other, and then how these interact to ultimately yield a measure of error between the two channels.

The question remains, however, "What does this mean in terms of what these channels are supposed to do?"

2.5 Channel Similarity Measure - Small Errors

Consider now the case of the error between two channels being small. We might reasonably expect this from well-designed hardware. Accordingly, with malice aforethought, we define a ratio of channel transfer functions as

$$R_{k,l}(f) = \frac{H_k(f)}{H_l(f)}. (37)$$

We stipulate for the analysis in this section that the difference between the transfer functions is relatively small, that is

$$\left|R_{k,l}(f)-1\right| << 1$$
, and $\left|R_{l,l}(f)\right| = 1$. (38)

The tacit assumption is that $H_l(f)$ exhibits no nulls in the passband. Again, this does not seem to be unreasonable for well-designed hardware.

This means we can write one transfer function in terms of the other as

$$H_k(f) = R_{k,l}(f)H_l(f). \tag{39}$$

Using this with Eq. (32) and Eq. (37) allows us to write the Figure of Merit as

$$FOM = \frac{\text{Re}\{R_{k,l}(f)\}}{\text{Re}\{R_{k,l}(f)\} + \frac{1}{2} |R_{k,l}(f) - 1|^2},$$
(40)

which can for small errors be approximated as

$$FOM \approx 1 - \left(\operatorname{Re}\left\{R_{k,l}(f)\right\} - 1\right)^{2}.$$
(41)

The adequacy of this approximation depends on just how small really is the initial imbalance, whether by design or some degree of preliminary calibration. Nevertheless, it gets more accurate the closer we get to balancing the channels of interest.

Recall that this FOM reaches its maximum value of one only when $R_{k,l}(f) = 1$, that is, when both channels are identical in both amplitude and phase.

Now, we also stipulate that the ratio of transfer functions may be written as

$$R_{k,l}(f) = \frac{H_k(f)}{H_l(f)} = \frac{H_k(f)\bar{H}_l(f)}{|H_l(f)|^2}.$$
(42)

We also observe the following property that will be useful later, namely

$$R_{k,l}(f)|H_l(f)|^2 = \overline{R}_{l,k}(f)|H_k(f)|^2.$$
 (43)

One nice feature of the ratio of transfer functions is that it can be calculated from the channel outputs when the channels are input with a common signal. That is, let

$$Y_{k,common}(f) = H_k(f)X_{common}(f), \text{ and}$$

$$Y_{l,common}(f) = H_l(f)X_{common}(f).$$
(44)

Then we may calculate the ratio of transfer functions as

$$\frac{Y_{k,common}(f)}{Y_{l,common}(f)} = \frac{H_k(f)X_{common}(f)}{H_l(f)X_{common}(f)} = \frac{H_k(f)}{H_l(f)} = R_{k,l}(f). \tag{45}$$

Virtually any broadband input signal $X_{common}(f)$ may be used, with the stipulation that it contain no nulls in the passband.

2.6 Matched Filter Analysis

We now consider the concept of a matched filter. Its development and attributes are well documented in the literature. We repeat some of attributes here.

- 1. The matched filter, when input with a signal to which it is matched, will output a signal that is the autocorrelation function of that signal.
- 2. The matched filter is optimal in the sense of maximizing Signal-to-Noise Ratio (SNR) of the output, when the input is in the presence of Additive White Gaussian Noise (AWGN).

Treating the channel as a filter, the signal to which a channel/filter is matched is identified as

$$X_{k}(f) = C_{k}\overline{H}_{k}(f), \tag{46}$$

where

$$C_k$$
 = some arbitrary scaling constant across the passband. (47)

The output of the channel with specific matched input is

$$Y_{k,k}(f) = C_k H_k(f) \overline{H}_k(f) = C_k \left| H_k(f) \right|^2. \tag{48}$$

We are tacitly assuming that this is true over some limited band of interest, and outside that band we really don't care too much.

Now consider that we have two channels, for each of which we identify a corresponding matched input signal. Now consider that we apply each of those inputs to the other channel, so that we generate specific outputs

$$Y_{k,k}(f) = C_k |H_k(f)|^2,$$

$$Y_{l,l}(f) = C_l |H_l(f)|^2,$$

$$Y_{k,l}(f) = C_l H_k(f) \overline{H}_l(f), \text{ and}$$

$$Y_{l,k}(f) = C_k H_l(f) \overline{H}_k(f).$$

$$(49)$$

With appropriate substitutions, including Eq. (37), we have

$$Y_{k,l}(f) = C_l |H_l(f)|^2 \left(\frac{H_k(f)}{H_l(f)}\right) = Y_{l,l}(f) R_{k,l}(f).$$
(50)

Furthermore, the other channel output can be written as

$$Y_{l,k}(f) = C_k \left| H_k(f) \right|^2 \left(\frac{H_l(f)}{H_k(f)} \right) = \left[\frac{C_k}{C_l} \left| R_{k,l} \right|^2 \right] \frac{1}{Y_{kl}(f)}. \tag{51}$$

Nevertheless, quite simply from Eq. (50), we may interpret that the mismatched channel output is simply a filtered version of the matched channel output, with the new filter just being a ratio of the respective channel transfer functions $R_{k,l}(f)$.

Recall that our earlier figure of merit for small errors remains approximately

$$FOM \approx 1 - \left(\text{Re} \left\{ R_{k,l}(f) \right\} - 1 \right)^2 = 1 - \left(\text{Re} \left\{ \frac{Y_{k,l}(f)}{Y_{l,l}(f)} - 1 \right\} \right)^2.$$
 (52)

Our figure of merit is then essentially a function of the magnitude of the mismatched channel output normalized to a matched channel output, and of course related directly to their respective channel transfer functions.

Recognizing that each transfer function has a corresponding impulse response, we identify

$$y_{l,l}(t) \Leftrightarrow Y_{l,l}(f)$$
, and $r_{k,l}(t) \Leftrightarrow R_{k,l}(f)$. (53)

This allows us to write the corresponding time-domain filtering operation as

$$y_{k,l}(t) = r_{k,l}(t) * y_{l,l}(t). (54)$$

2.6.1 Desired Attributes

For matched filters/channels, we obviously desire that over the passband of interest we have an ideal response, that is

$$R_{k,l}(f) = \operatorname{rect}\left(\frac{f - f_k}{B_k}\right) = \operatorname{rect}\left(\frac{f - f_l}{B_l}\right),$$
 (55)

and the corresponding impulse response to be

$$r_{k,l}(t) = B_k \operatorname{sinc}(B_k t) e^{j2\pi f_k t}.$$
(56)

Of special note to us is that we desire for the magnitude of the ratio's impulse response

$$\left|r_{k,l}(t)\right| = B_k \left|\operatorname{sinc}(B_k t)\right|. \tag{57}$$

2.6.2 Amplitude vs. Phase Effects

The ratio of transfer functions may be written in a manner so that we can separately identify amplitude and phase effects. That is, we may write

$$R_{k,l}(f) = R_{amplitude,k,l}(f)R_{phase,k,l}(f), \tag{58}$$

where we can individually identify

$$R_{amplitude,k,l}(f) = \frac{A_k(f)}{A_l(f)} \operatorname{rect}\left(\frac{f - f_k}{B_k}\right), \text{ and}$$

$$R_{phase,k,l}(f) = e^{j(\Phi_k(f) - \Phi_l(f))} \operatorname{rect}\left(\frac{f - f_k}{B_k}\right), \tag{59}$$

where we have made the implicit assumption of identical passbands, that is

$$\operatorname{rect}\left(\frac{f - f_k}{B_k}\right) = \operatorname{rect}\left(\frac{f - f_l}{B_l}\right). \tag{60}$$

Separating amplitude and phase contributions can be useful when specifying channel matching requirements when we have different levels of control for mitigating the effects of imbalance with respect to phase versus amplitude.

Important parameters in channel balance measurement are the relative phase difference and the relative group delay between channels. We now define corresponding measures as

$$\phi_{k,l} = \Phi_k(f_k) - \Phi_l(f_k) = \text{nominal relative phase difference, and}$$

$$\tau_{k,l} = \left\langle -\frac{1}{2\pi} \frac{d}{df} (\Phi_k(f) - \Phi_l(f)) \right\rangle = \text{mean relative group delay.}$$
(61)

where $\langle \ \rangle$ denotes mean value, with the tacit assumption that the phase difference is "unwrapped," that is, does not contain any 2π jumps.

2.7 Comparing Channels to Ideal

Here we ask the question for any one channel "How close is the channel to ideal?"

Recall that the ideal channel was characterized in Section 2.2, specifically by Eq. (16) and Eq. (17). We accordingly identify

$$R_{k,ideal}(f) = R_{amplitude,k,ideal}(f)R_{phase,k,ideal}(f), \tag{62}$$

where we can individually identify

$$R_{amplitude,k,ideal}(f) = \frac{A_k(f)}{C_{ideal}} \operatorname{rect}\left(\frac{f - f_{ideal}}{B_{ideal}}\right), \text{ and}$$

$$R_{phase,k,ideal}(f) = e^{j(\Phi_k(f) + 2\pi T_{ideal}f)} \operatorname{rect}\left(\frac{f - f_{ideal}}{B_{ideal}}\right),$$
(63)

where we have assumed the same passbands, that is

$$\operatorname{rect}\left(\frac{f - f_k}{B_k}\right) = \operatorname{rect}\left(\frac{f - f_{ideal}}{B_{ideal}}\right). \tag{64}$$

This allows us explicitly to write the ratio of transfer functions as

$$R_{k,ideal}(f) = \frac{e^{j2\pi T_{ideal}f}}{C_{ideal}} H_k(f). \tag{65}$$

The corresponding impulse response is

$$r_{k,ideal}(f) = \left(\frac{1}{C_{ideal}}\right) \delta(t + T_{ideal}) * h_k(t).$$
(66)

Note that the shape of the ratio is determined by the channel filter function $H_k(f)$. The ratio impulse response is merely a scaled and shifted version of $h_k(t)$, with the amounts of scale and/or shift having been predetermined to adjust for whatever is "ideal."

Recall the nature of $h_k(t)$ is such that we would expect a relatively strong peak shifted in time from t=0. For an ideal channel it would be a sinc function. For a non-ideal channel we expect a perturbation from the sinc function due to real hardware being composed of non-ideal components. The most obvious effects in $h_k(t)$ will generally be observed in

- 1. A broadening of the mainlobe,
- 2. An undesirable scaling in mainlobe amplitude,
- 3. A shifting in time of the mainlobe, and
- 4. An amplification of the sidelobes.

That these features are readily observable in $h_k(t)$, and largely distinct from each other, makes the impulse response particularly attractive for assessing channel/filter performance. We stipulate that low-level sidelobe structure might (read that as "probably will") require data tapering (window functions) be applied prior to impulse response calculations. There are a plethora of window taper functions from which to choose.¹

In any case, the impulse response measure integrates many of the aspects of the transfer function, obviating requirements for, say, quadratic phase error, cubic phase error, random phase errors, and ripple in both amplitude and phase across the passband.

A discussion of various channel errors impact on the IPR is given in a previous report by Doerry.²

2.8 Comparing Channels to Each Other

From section 2.6.2, we recall the ratio of transfer functions may be written as

$$R_{k,l}(f) = R_{amplitude,k,l}(f)R_{phase,k,l}(f), \tag{67}$$

where we can individually identify

$$R_{amplitude,k,l}(f) = \frac{A_k(f)}{A_l(f)} \operatorname{rect}\left(\frac{f - f_k}{B_k}\right), \text{ and}$$

$$R_{phase,k,l}(f) = e^{j(\Phi_k(f) - \Phi_l(f))} \operatorname{rect}\left(\frac{f - f_k}{B_k}\right), \tag{68}$$

where we have made the implicit assumption that

$$\operatorname{rect}\left(\frac{f - f_k}{B_k}\right) = \operatorname{rect}\left(\frac{f - f_l}{B_l}\right). \tag{69}$$

Specific phase attributes are

$$\phi_{k,l} = \Phi_k(f_k) - \Phi_l(f_k) = \text{nominal relative phase difference, and}$$

$$\tau_{k,l} = \left\langle -\frac{1}{2\pi} \frac{d}{df} (\Phi_k(f) - \Phi_l(f)) \right\rangle = \text{mean relative group delay.}$$
(70)

We will calculate the corresponding impulse response as

$$r_{k,l}(t) \Leftrightarrow R_{k,l}(f).$$
 (71)

Our measures will be with respect to the impulse response $r_{k,l}(t)$. We again stipulate that low-level sidelobe structure might (read that as "probably will") require data tapering (window functions) be applied prior to impulse response calculations.

2.9 Relationship to Coherence Measure

Recall that we may write the ratio functions as

$$R_{k,l}(f) = \frac{H_k(f)\overline{H}_l(f)}{\left|H_l(f)\right|^2}, \text{ and}$$

$$R_{l,k}(f) = \frac{H_l(f)\overline{H}_k(f)}{\left|H_k(f)\right|^2}.$$
(72)

Taking the expected values (over frequency) of numerators separately from denominators yields the ratio functions of expected values as

$$P_{k,l} = \frac{\left\langle H_k(f)\overline{H}_l(f) \right\rangle}{\left\langle \left| H_l(f) \right|^2 \right\rangle}, \text{ and}$$

$$P_{l,k} = \frac{\left\langle H_l(f)\overline{H}_k(f) \right\rangle}{\left\langle \left| H_k(f) \right|^2 \right\rangle}.$$
(73)

In typical systems, we would expect the amplitudes of these quantities to be very near each other, but phase to be opposite. Taking the geometric mean of one result with the conjugate of the other result yields

$$\rho_{k,l} = \sqrt{P_{k,l} \overline{P}_{l,k}} \ . \tag{74}$$

We have used the complex conjugate so as to not destroy the phase difference contribution.

Nevertheless, we identify this as the complex coherence measure, expanded and summarized as

$$\rho_{k,l} = \frac{\left\langle H_k(f) \overline{H}_l(f) \right\rangle}{\sqrt{\left\langle \left| H_k(f) \right|^2 \right\rangle \left\langle \left| H_l(f) \right|^2 \right\rangle}} \,. \tag{75}$$

We further note its relationship to the complex conjugate of the transposition of functions as

$$\rho_{k,l} = \overline{\rho}_{l,k} \,. \tag{76}$$

An important point is that the coherence measure is about expected values, and is not a point measure, as for a single frequency.

At a single frequency, the expected values become the point frequency response of the channels themselves, and the coherence measure is simply a unit-modulus phasor.

Returning to our normalized error measure of Eq. (28), had this been written in terms of expected values, then Eq. (30) would result in a single number, and could be written as

$$\eta = 1 - \left\lceil \frac{G_{k,l}}{M_{k,l}} \right\rceil \operatorname{Re} \left\{ \rho_{k,l} \right\}. \tag{77}$$

where we now define with respect to expectations over spectral densities

$$G_{k,l} = \sqrt{\left\langle \left| H_k(f) \right|^2 \right\rangle \left\langle \left| H_l(f) \right|^2 \right\rangle} = \text{geometric mean, and}$$

$$M_{k,l} = \frac{\left\langle \left| H_k(f) \right|^2 \right\rangle + \left\langle \left| H_l(f) \right|^2 \right\rangle}{2} = \text{arithmetic mean.}$$
(78)

In any case, since the coherence measure is over a frequency band, it has lost the ability to represent any overt detailed frequency-dependence.

That is not to say that coherence is not a useful number as a succinct expression of channel matching. We merely state that it does not help us to identify just what exactly is different about the two channels, at least within the band over which expected values are calculated.

It is entirely reasonable, however, to calculate coherence over frequency sub-bands, to gain some degree of frequency-dependence for a corresponding comparative analysis.

Nevertheless, consistent with Eq. (32), we might offer the concept of an "integrated" Figure of Merit as

$$FOM_{integrated,k,l} = \left[\frac{G_{k,l}}{M_{k,l}}\right] \operatorname{Re}\left\{\rho_{k,l}\right\}. \tag{79}$$

Clearly, while this FOM is a strong function of coherence, it is also adversely affected by differences between geometric and arithmetic means, which occurs when channel gains are not equal.

We also point out that the heretofore assumption of Time-Invariance implies that we have perfect coherence for any single channel with itself over time.

An excellent discussion of coherence for Synthetic Aperture Radar (SAR) images is given by Bickel,³ and using coherence as a measure of goodness for SAR image compression is offered by Bickel and Doerry.⁴ This paper shows the utility of regional coherence measures.

2.10 Ideal Nonlinear Channels

We now abandon the notion of a linear channel, in the sense that it is common for receiver channels to employ frequency conversion; translation to/from intermediate frequency bands or basebands, for easier data processing. In such systems, the passband into the receiver channel is not the same passband out of the receiver channel; frequency translations and sometimes frequency multiplications occur.

Strictly speaking, transfer functions defined based on LTI systems no longer apply. However, Eq. (45) provides a path forward to allow analysis by the techniques in sections 2.7 and 2.8. That is, if we employ a common input signal, then all we need to do is with brilliant obviousness compare the outputs of the two channels to each other to evaluate their balance, regardless of the mixing, multiplying, or other circuit functions present along the way in the individual channels.

2.11 Secondary Issues

Heretofore we have focused on channel gain functions to signals that are input to them. However, other characteristics of multi-channel systems can also have important impact on overall system performance. We mention here some additional issues to be considered when comparing multiple channels with each other.

2.11.1 Noise Floor

Optimal processing across channels assumes known, and generally equal, background noise levels in the various channels. Ideally, the noise floor is at theoretically minimum levels, unless specifically designed to be otherwise.⁵ If subsequent processing was to assume equal noise statistics on all relevant channels, when in fact we don't have that, the result may be suboptimal processing results, and perhaps unacceptable biases in relative calculations.

Consequently, we desire equal noise spectral statistics, in both shape and level, between all channels. This is especially true for broadband background noise. While noise spectra should exhibit equal statistics, preferably broadband and white, the noise should nevertheless be uncorrelated between channels, lest the noise bias actual signal measurements.

In addition to broadband background noise, a channel may exhibit decidedly non-white spurious content. These often manifest as interfering signals, affecting the fidelity of renderings of the radar data, e.g. range/Doppler images; capable of being detected as false alarms.

2.11.2 Nonlinear Distortions

If any individual channel exhibits nonlinear gain characteristics, then the result is often the generation of harmonic content and mixing products, i.e. spurious signal content of a multiplicative nature. These are, of course, undesirable. A principal source of such nonlinear gain characteristics is an Analog to Digital Converter (ADC).^{6,7} We further note that the relative spurious signal levels are often dependent on input signal levels in a very nonlinear manner; they scale in unpredictable ways. Consequently, signal dynamic range is an important factor.

Effects of nonlinear distortions are especially important for radar modes that exhibit large integration gains but still wish to detect signals down near the noise level, such as with high-performance GMTI radar systems.⁸

2.11.3 Crosstalk

The typical, and ideal, assumption is that each channel processes only its own desired input. That is, the output of channel k is not influenced by the signal in channel l.

Of course, this is ideal, and we are never quite so fortunate. The ability of a signal in one channel to leak, or couple, to another channel is termed "cross-talk." As such, it can be considered a noise source that is highly correlated with a signal in another channel. Clearly, if signals in separate channels are expected to be orthogonal, cross-talk obviously diminishes that orthogonality.

2.12 Frequency Sampling Issues

Our fundamental input measurement for ascertaining channel balance is likely to be a sampled version of the transfer function; sampled at evenly spaced frequencies over the passband of interest. The granularity of the frequency samples will determine the unambiguous span of time-delays which we might calculate. This is strictly a sampling-theory issue, but with frequency-sample-spacing. Accordingly

$$\tau_{\text{max}} = \frac{1}{\Delta f} = \text{maximum unambiguous group delay},$$
 (80)

where

$$\Delta f$$
 = frequency sample spacing. (81)

3 Examples of Imbalance Effects

We now examine qualitatively several applications of multiple channels, and the effects of channel imbalance on those applications.

3.1.1 Monopulse Antenna

Monopulse antennas are used extensively in tracking radars, and for Direction of Arrival (DOA) measurements. An excellent text on these antennas is by Sherman and Barton.⁹ Recall that monopulse channels may originate from separate antenna beam feeds, but are typically transmogrified to sum and difference channels by circuitry often referred to as a "comparator." Other names include "monopulse-network," "hybrid," and "magic-T."

The following examples are from data taken by the Sandia National Laboratories Ka-band along-track phase monopulse FARAD test-bed radar system of a grass park scene. Figure 2 shows a SAR image from the sum channel of the site used for the examples in this section. This image is convenient for this report for illustrating monopulse issues because of the uniformity of the clutter.



Figure 2. Ka-band SAR image of grass park from SNL FARAD system.

The following example is of a short coherent processing interval (coarse azimuth) range-Doppler image of this same area. The sum channel image is shown below of a grass park in Figure 3 and the difference channel image is shown in Figure 4.

The monopulse ratio for each pixel is shown in Figure 5. Since this is a phase monopulse system, the direction-of-arrival information is contained in the imaginary part of the monopulse ratio. Figure 6 details a mean value across the range direction. This will serve as reference for the following discussion. Of significance is that the real part of the ratio is essentially zero, and the imaginary part is essentially linear with negative slope, crossing zero at approximately pixel index 129.

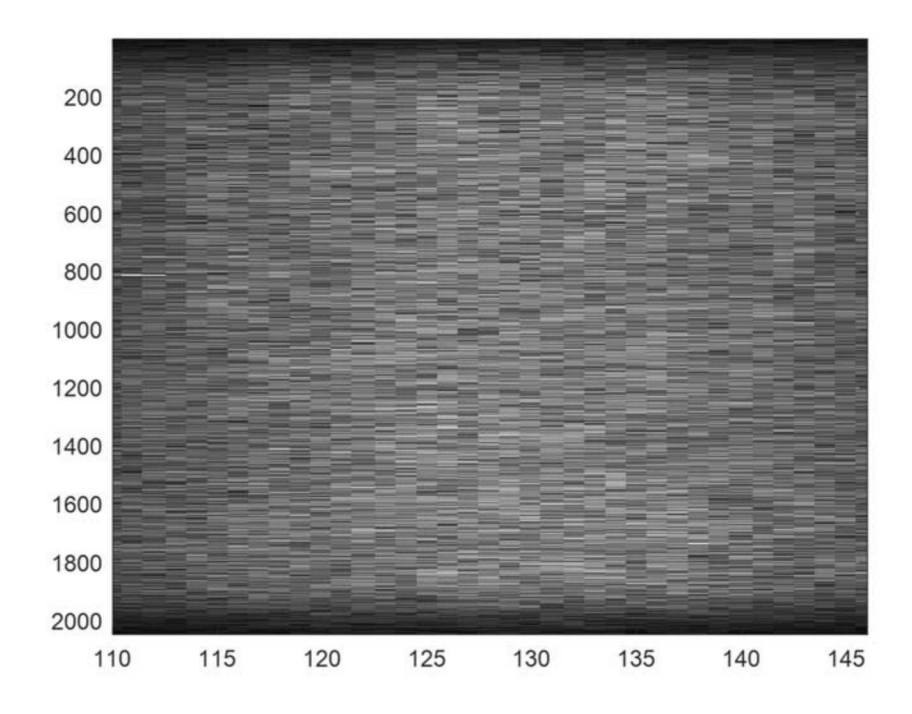


Figure 3. Sum image of a grass park region from a Ka-band monopulse radar.

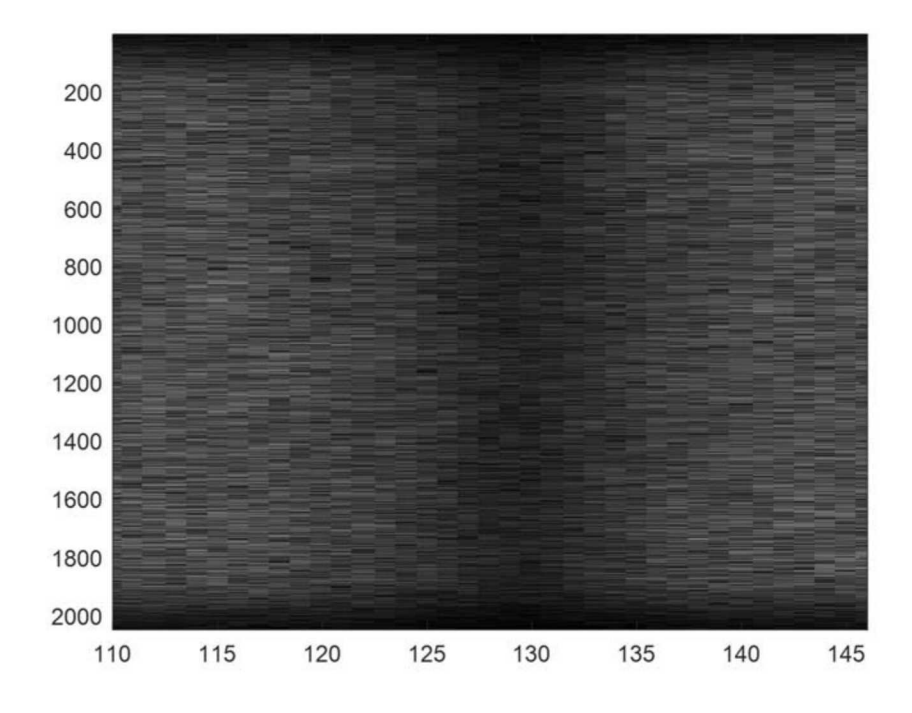


Figure 4. Difference image of a grass park region from a Ka-band monopulse radar.

In the following sections we illustrate the effects of amplitude and phase errors that are introduced before (pre-comparator) and after (post-comparator) the formation of the sum and difference beams. More information on the general effects of pre-comparator and post-comparator errors are presented in another report. Unless these errors are detected and corrected, they distort the relationship between the monopulse ratio and estimated angle-of-arrival.

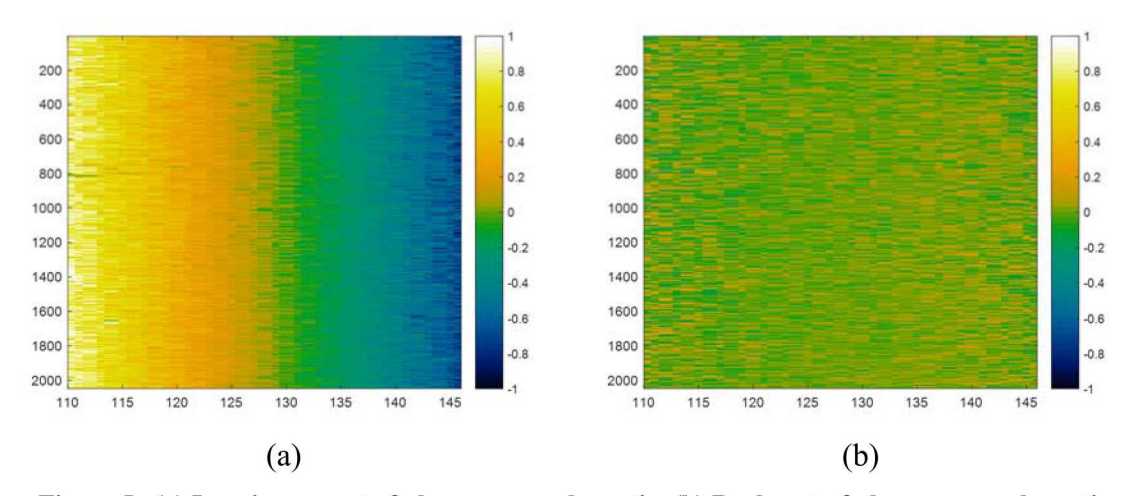


Figure 5. (a) Imaginary part of phase monopulse ratio, (b) Real part of phase monopulse ratio.

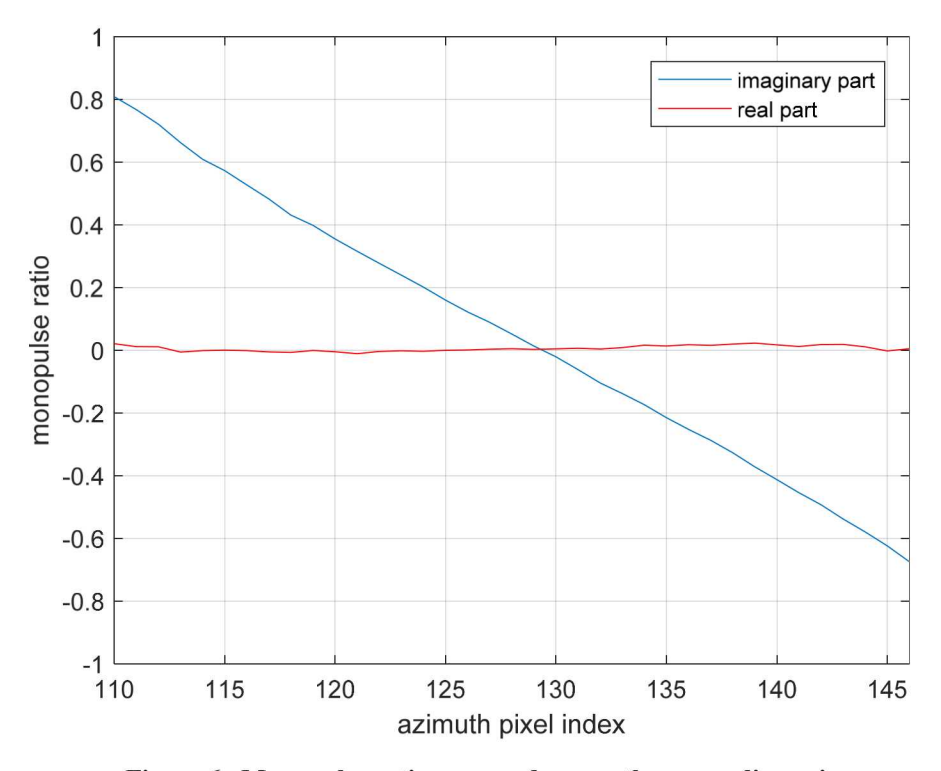


Figure 6. Monopulse ratio averaged across the range dimension.

Pre-comparator errors

As the name implies, pre-comparator errors are imbalances and error effects that occur before the comparator sums and differences the individual beams. Figure 7 and Figure 8 show the error from a pre-comparator amplitude error of about 1 dB. These errors tend to distort the null-depth and location.

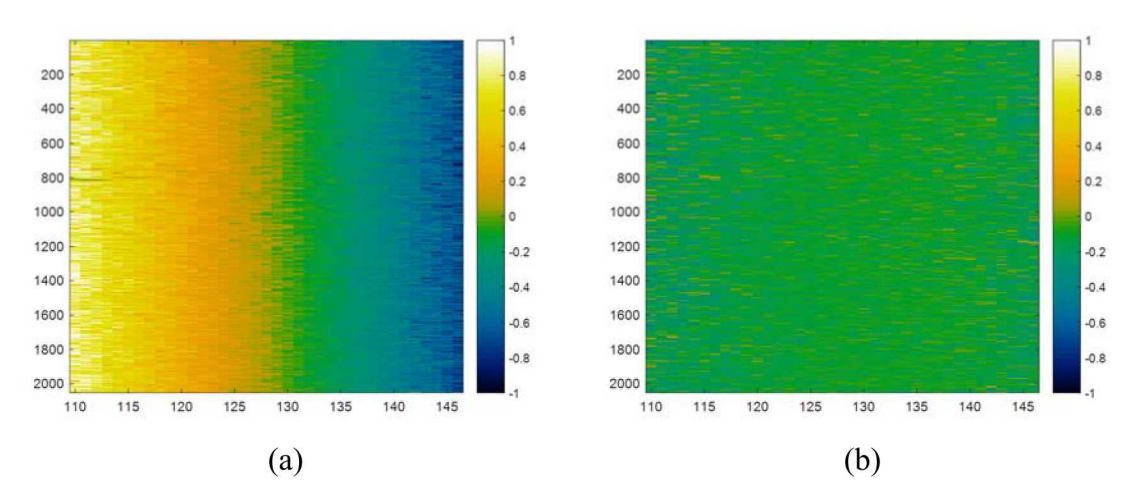


Figure 7. (a) Imaginary part of monopulse ratio with pre-comparator amplitude error, (b) Real part of monopulse ratio with pre-comparator amplitude error.

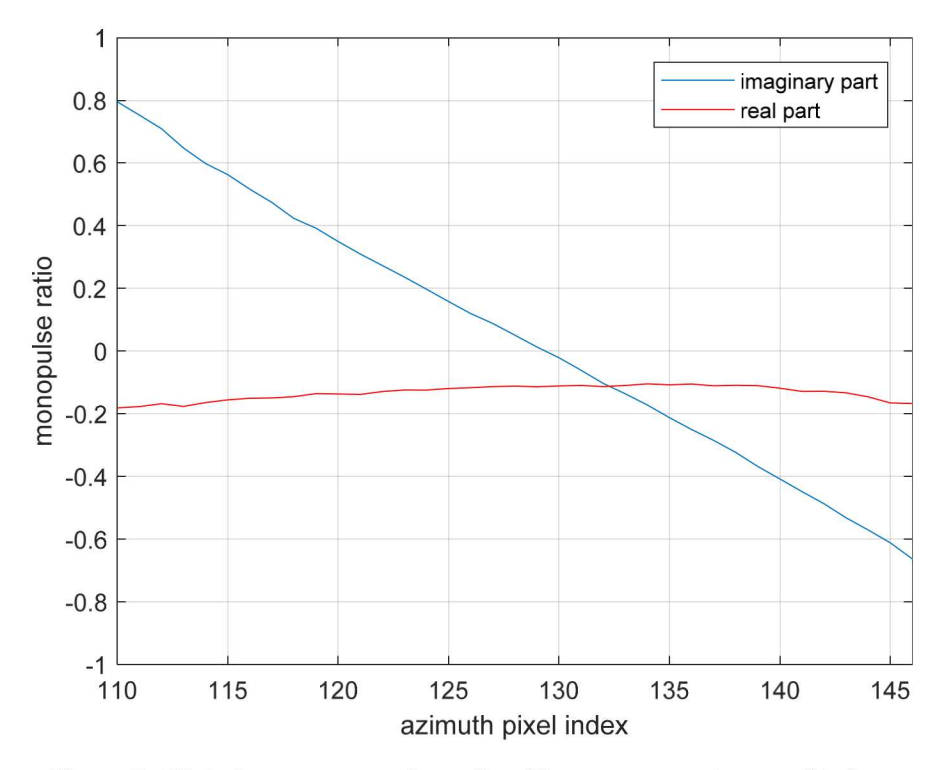


Figure 8. Plot of mean monopulse ratio with pre-comparator amplitude error.

A pre-comparator phase error will similarly degrade the null location. Figure 9 and Figure 10 show the error from a pre-comparator phase error of 45°.

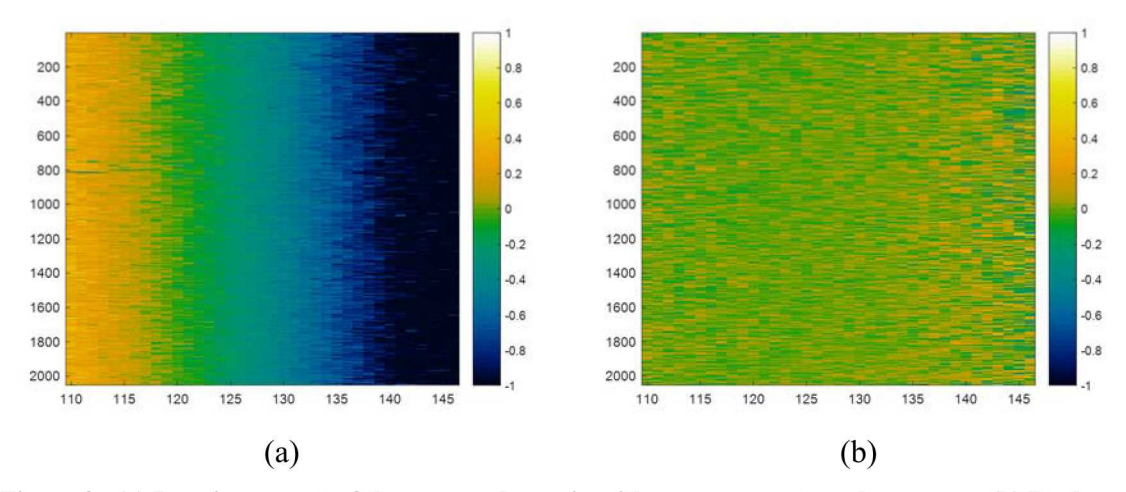


Figure 9. (a) Imaginary part of the monopulse ratio with pre-comparator phase error, (b) Real part of monopulse ratio with pre-comparator phase error.

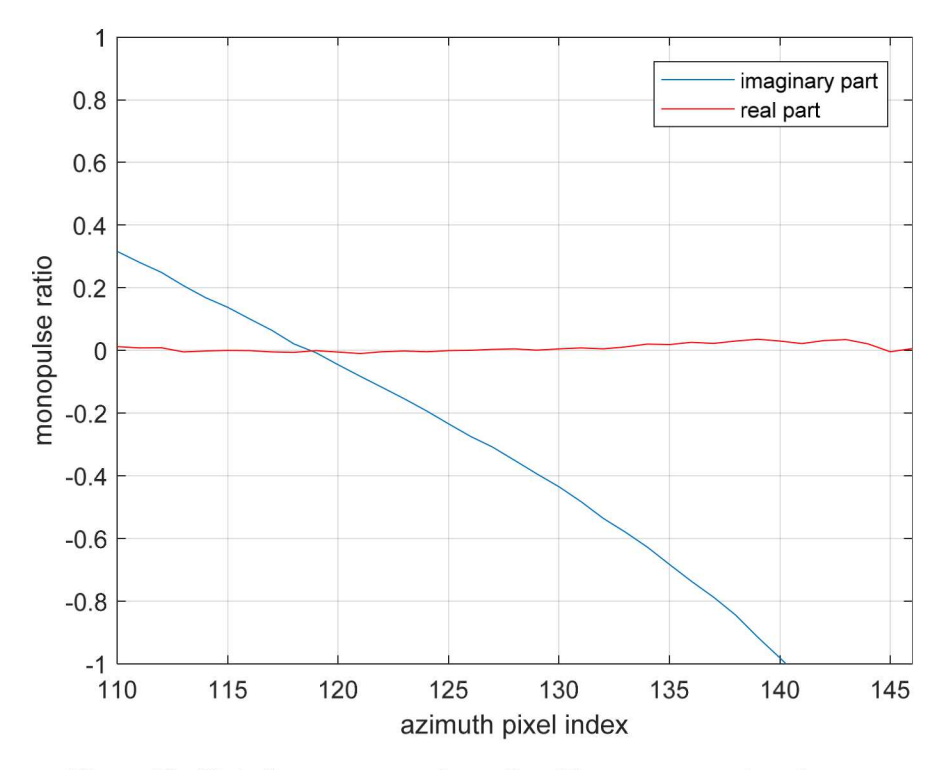


Figure 10. Plot of mean monopulse ratio with pre-comparator phase error.

Post-comparator errors

Figure 11 and Figure 12 show the error from a post-comparator amplitude error of about 1 dB. A post-comparator amplitude error scales the monopulse ratio which in turn yields a scaling error in the estimated direction-of-arrival.

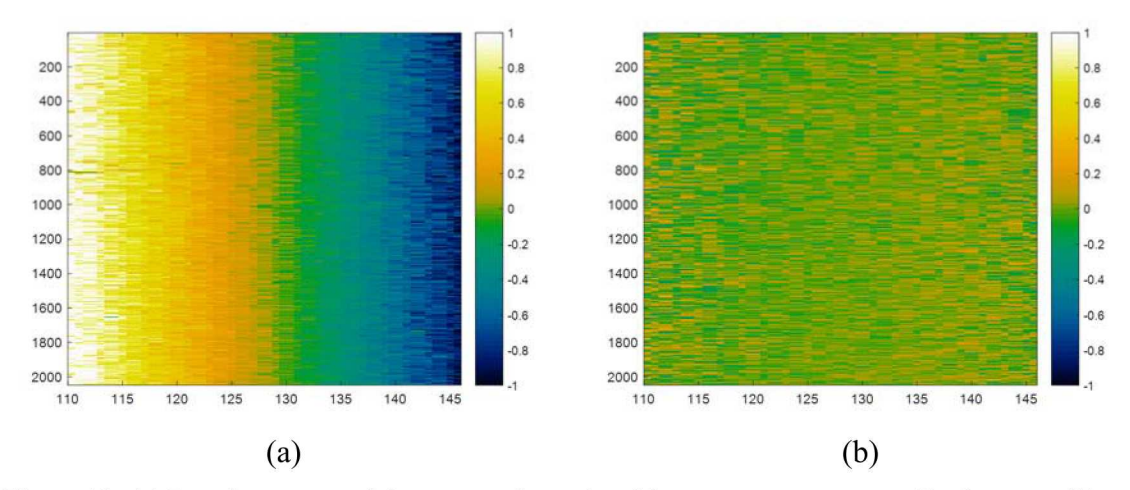


Figure 11. (a) Imaginary part of the monopulse ratio with post-comparator amplitude error, (b) Real part of the monopulse ratio with post-comparator amplitude error.

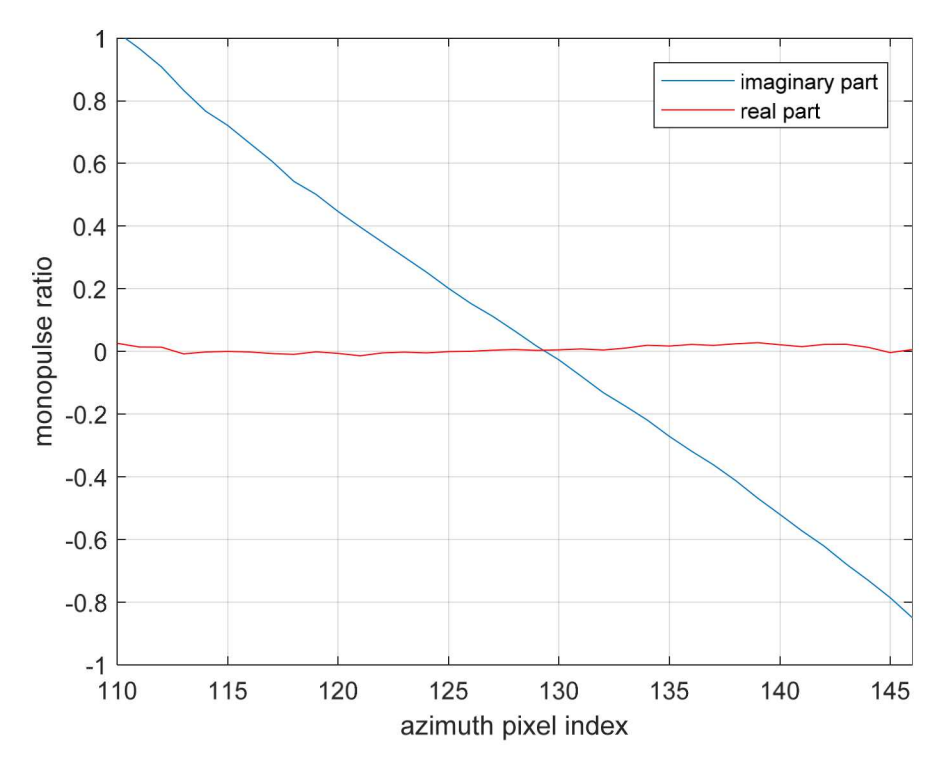


Figure 12. Mean monopulse ratio with post-comparator amplitude error.

The post-comparator phase error rotates the monopulse ratio information from the imaginary (from phase monopulse) channel to the real channel which scales the monopulse ratio relative to the direction-of-arrival estimates. Figure 13 and Figure 14 show the error from a post-comparator phase error.

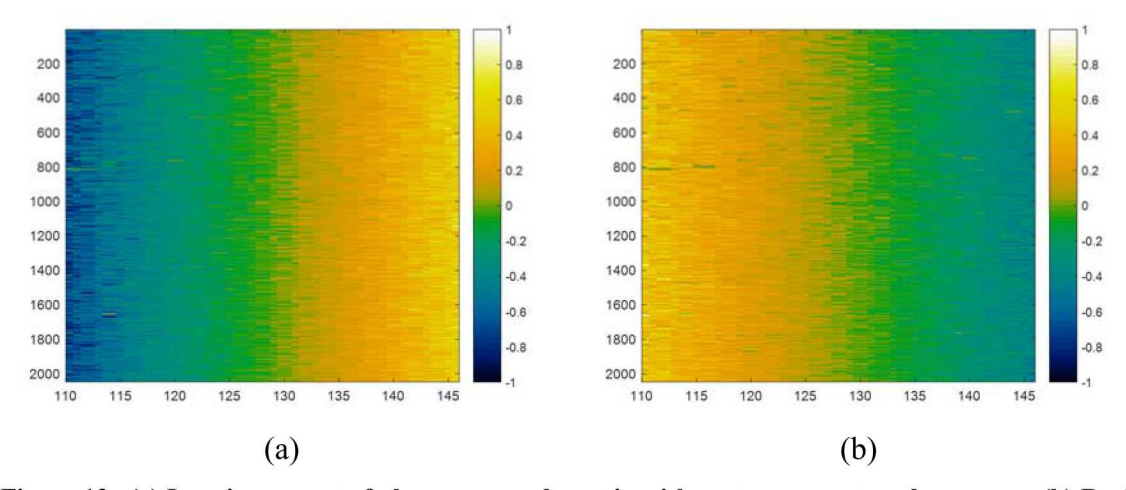


Figure 13. (a) Imaginary part of phase monopulse ratio with post-comparator phase error, (b) Real part of phase monopulse ratio with post-comparator phase error.

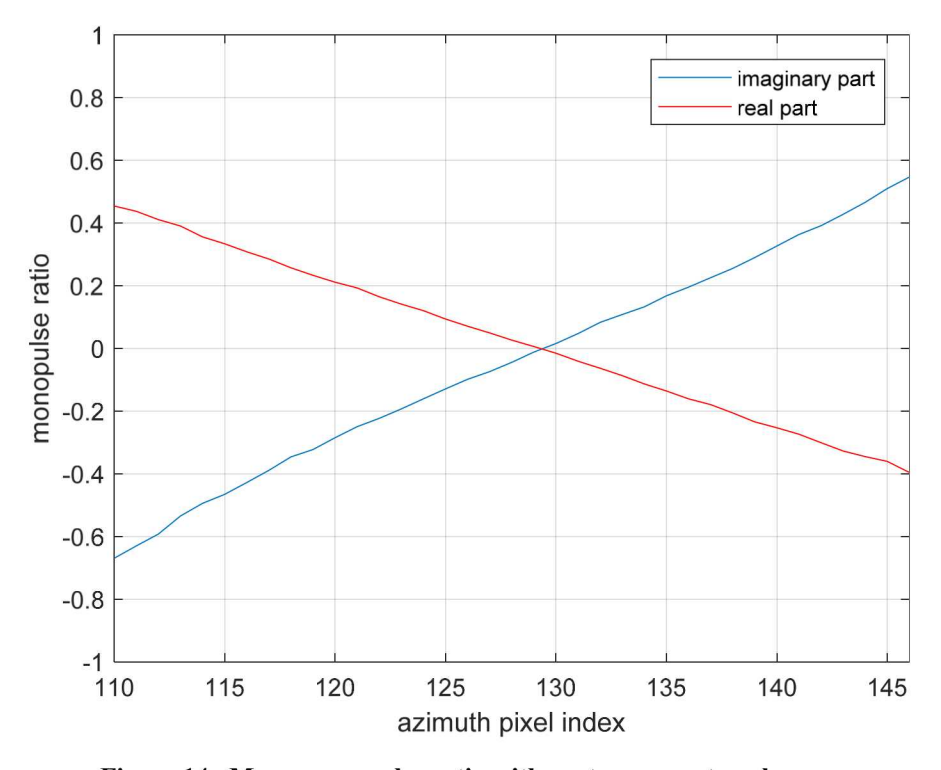


Figure 14. Mean monopulse ratio with post-comparator phase error.

3.1.2 Clutter Cancelling GMTI

In clutter cancellation, uncorrected phase, amplitude, and group delay lead to loss in cancellation performance.

Figure 15 shows the short CPI sum image of a region of clutter, where pixel brightness is in units of decibels (dB). Figure 16 is the clutter cancelled image of the same area also in dB. Errors in cancellation will cause an increase in the residual clutter level which will interfere with target detection.

We now show the effect on cancellation of several uncorrected channel-matching errors. Figure 17 illustrates the effects on clutter cancellation from a 1-dB amplitude error, whereas Figure 18 illustrates the effects on clutter cancellation from a 30-degree phase error. Figure 19 shows the effects of an error in matching group delay.

Gierull¹¹ presents and reports results for using two techniques for balancing 2-channel GMTI data; one for phase only, and one that includes magnitudes.

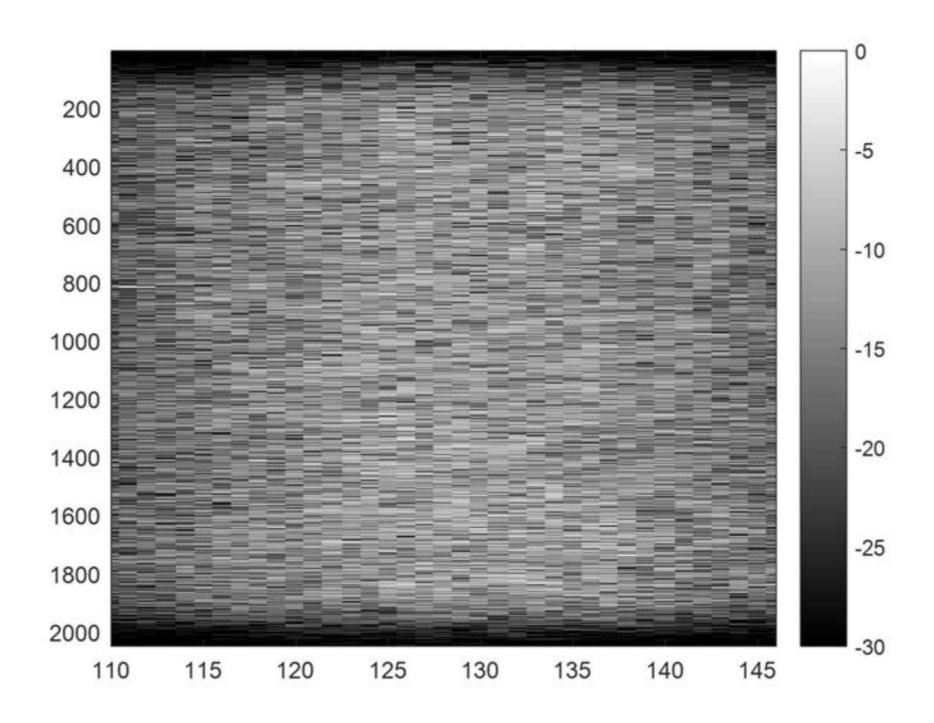


Figure 15. Section of range-Doppler image of uniform clutter.

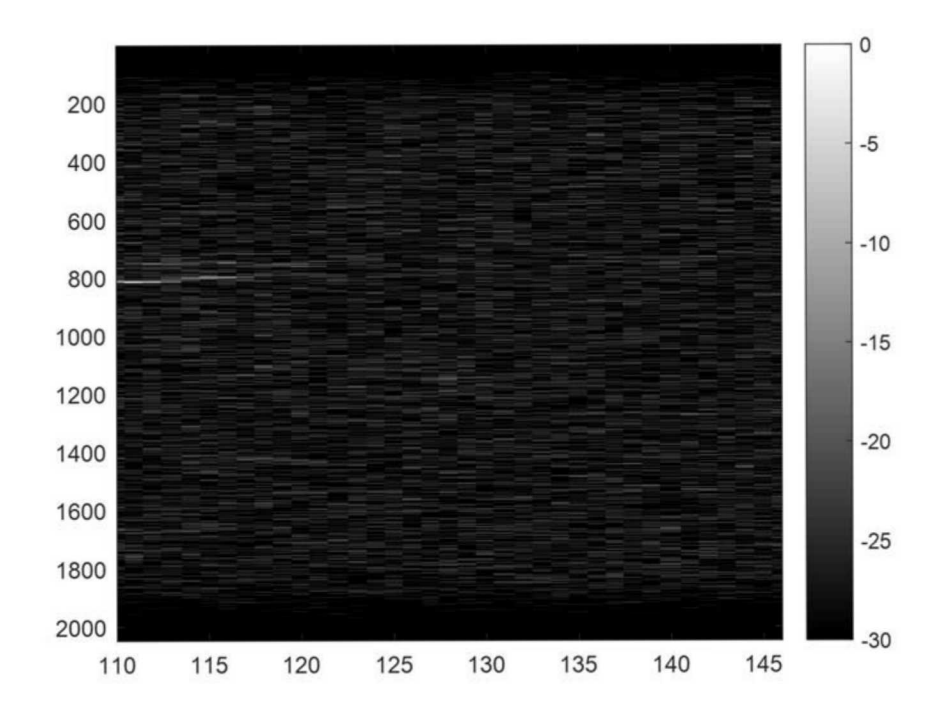


Figure 16. Reference clutter-cancelled image (mean ~-26.7 dB).

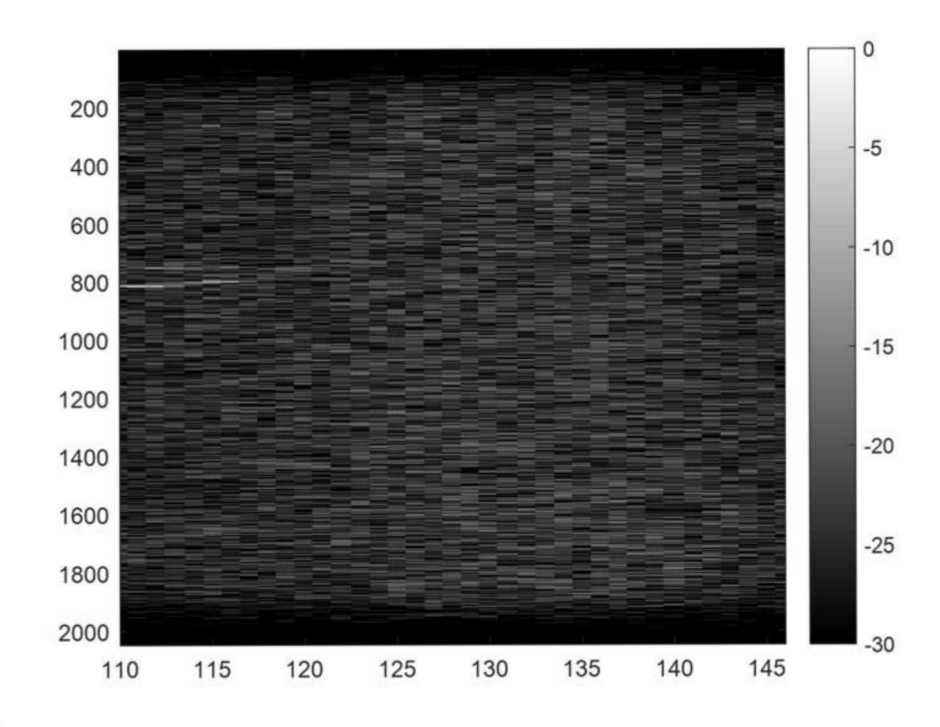


Figure 17. Clutter cancellation performance for 1 dB amplitude error (mean ~-21.7 dB).

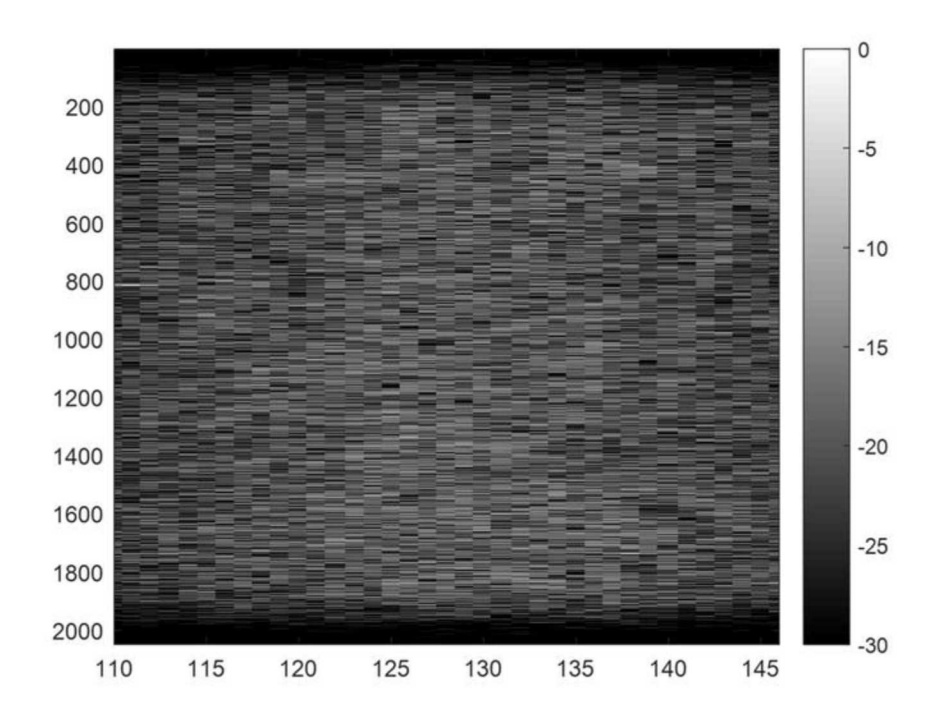


Figure 18. Clutter cancellation performance for uncompensated 30-degree phase error (mean ~-17.8 dB).

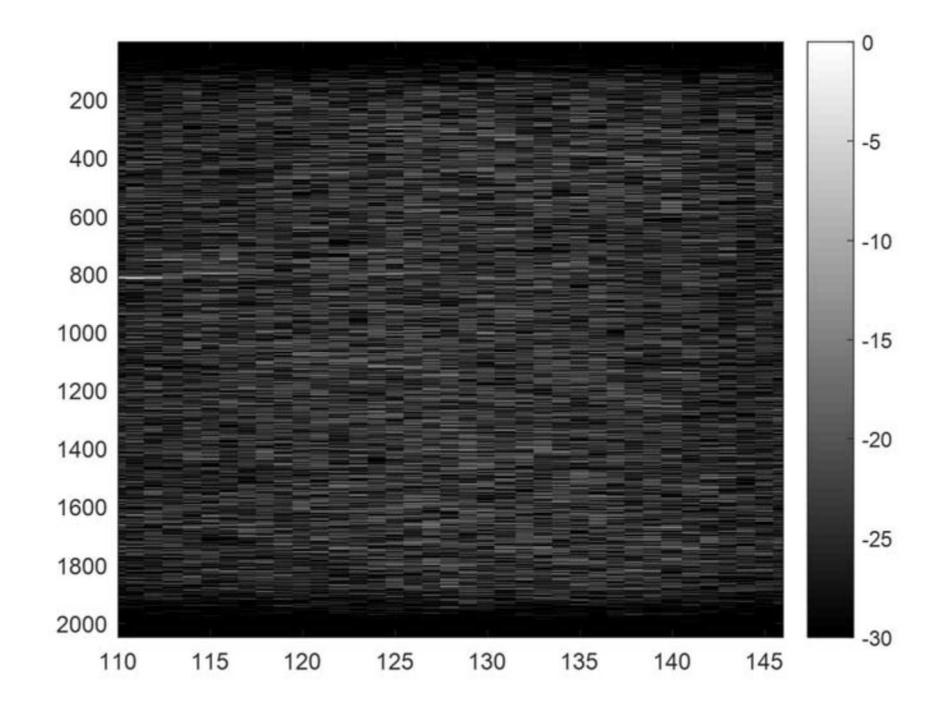


Figure 19. Clutter attenuation due to group delay (mean ~-22.2 dB).

3.1.3 Interferometric SAR

In Interferometric-SAR (IFSAR, InSAR), calibration errors in phase introduce errors in the estimated terrain topography. A discussion of height error sources is given in an earlier report. Amplitude calibration errors are less important for IFSAR, but losses in SNR in one of the channels limits coherence, which in turn increases noise in the resulting terrain map. Group delay differences between the IFSAR channels introduces decorrelation, resulting in increased noise in the terrain estimate.

Bräutigam, et al., 13 discuss calibration of the TerraSAR-X and TanDEM-X bistatic orbiting-satellite IFSAR systems. Krieger, et al, 14 discuss the TanDEM-X with additional details.

3.1.4 Digital Beamforming (DBF)

In Digital Beamforming (DBF) applications, individual channels generally correspond to signal streams from separate antenna phase centers, or antenna beams. As such, channel errors are indistinguishable from signal modulations. The net results are unintended antenna beam sidelobes and sidelobe characteristics. Intended nulls based on calculations using desired or ideal antenna properties are no longer nulls in practice. This leads to reduced detection probabilities, and increased false alarm probabilities. This is in fact a generalization of the results exemplified in the previous section on clutter cancellation.

A popular technique for processing multiple-channel GMTI data is Space-Time Adaptive Processing (STAP).¹⁵ The intent of STAP processing is essentially to "learn" from the data and use data characteristics to optimize the detection and/or characterization of moving targets. However, the data embody both the effects of the channels as well as the nature of the environment that the radar is interrogating, and data processing is generally unable to separate them without additional information. Often, simplifying assumptions are made in lieu of additional information. However, simply attributing measurements to the environment while ignoring channel differences may lead to erroneous interpretations. Therefore, even in adaptive systems, channel balancing remains important.

Yang, et al., 16 discuss channel errors that affect Digital Beamforming.

Farquharson, et al., 17 offer a contrast-based calibration scheme for Digital Beamforming.

Younis, et al., ¹⁸ discuss multi-channel SAR system calibration. Younis, et al., ¹⁹ in another paper continues the discussion of DBF and SAR.

3.1.5 Polarimetric SAR

The desire of channel balance is to maintain polarization orthogonality of the signals in the polarization channels in order to measure target characteristics. As with the previous multiple-channel modes, we want to manage phase, amplitude, and delay differences between the channels. In addition, another important balance correction for multiple-channel radars is the cross-talk measurement and correction. There is more literature on the cross-talk correction for polarimetric radars than for other multiple channel radar system types. ^{20,21}

Freeman²² reviews the "development of algorithms for polarimetric radar calibration" and discusses "the problems involved in phase calibration of interferometric SAR."

3.1.6 Quadrature Demodulation

Modern high-performance radar systems often operate on the down-converted analytic representation of the received signal energy. The resulting baseband signal is complex-valued, itself represented with In-phase (I) and Quadrature (Q) values that often result from separate channels, or channel segments. To the extent that the I and Q channels are not identical, an imbalance may result, and often does.

Imbalance in I/Q channels results in nonorthogonality of their signals, causing leakage of 'image' frequencies into the data, further causing ghosting in radar range-Doppler maps resulting in false targets, often appearing similar to spurious signals.^{23,24}

4 How Good is Good Enough?

The question now at hand is "How well should receiver channels be balanced, both with respect to ideal, and with respect to each other?" Ultimately, this is an issue of signal purity.

Towards this end, we make some rather arbitrary statements below about to what degree channels should be balanced, with the caveat that we do not discourage the reader from developing more reasoned requirements derived from overall system performance requirements.

4.1 Comparing Channels to Ideal

Recall that the ideal channel was characterized in Section 2.2, specifically by Eq. (16) and Eq. (17). We offer that in the absence of specific derived requirements, any particular radar subsystem, or cascaded subsystems, be correctable to the following.

- 1. Impulse response mainlobe broadening less than 10 percent from ideal,
- 2. Impulse response mainlobe scaling be within 1 dB of ideal, for all system gain settings,
- 3. Group delay be measurable to less than 10 percent of the impulse response mainlobe width, and
- 4. Impulse response sidelobes less than -40 dBc, with respect to the impulse response mainlobe peak. This might be relaxed somewhat very near the mainlobe peak. This should be measurable with suitable data tapering.
- 5. Background noise should be white (flat spectrum) at theoretically justified levels; dictated by system noise figure allowances.
- 6. Any spurious signals, whatever the source, should be at a level below any detection threshold. In the absence of other criteria, spurious levels should be no more than 10 dB above the broadband noise floor, with statistical occurrence consistent with the allowable false-alarm rate.^{8,25}

4.2 Comparing Channels to Each Other

We offer that in the absence of specific derived requirements, any particular radar subsystem, or cascaded subsystems, be correctable to the following.

1. Ratio impulse response mainlobe broadening less than 10 percent from ideal,

- 2. Ratio impulse response mainlobe scaling be within 1 dB of each other, for all system gain settings,
- 3. Ratio impulse response mainlobe phase be less than 1 degree at mainlobe peak,
- 4. Group delay be less than 10 percent of the ratio impulse response mainlobe width, and
- 5. Ratio impulse response sidelobes be less than –40 dBc, with respect to the mainlobe peak. This might be relaxed somewhat very near the mainlobe peak. This should be measured with suitable data tapering.
- 6. Broadband noise spectral densities should be within 1 dB of each other for any channel pairs.
- 7. Crosstalk should meet the spurious signal requirements.
- 8. We offer that in the absence of specific derived requirements, any particular radar subsystem, or cascaded subsystems, be correctable to a coherence between channels better than 99 percent over the entire band or any sub-band.

4.3 Imbalance Mitigation Techniques

Channel balancing is a system issue, and needs to be dealt with from a systems standpoint. Most importantly, mitigation of channel imbalances should not be an afterthought. It is a poor system design strategy to address channel balance with "Oh, we're not going to worry about it now, and just take care of it in software, later."

Achieving good channel balance will generally require a collaboration of several techniques. We next examine a hierarchy of several techniques.

1. Prevent Imbalance

We note that any imbalance that can be prevented doesn't have to be dealt with later. Consequently, we begin with proper component selection, and circuit design/construction. This may necessitate, or at least be aided by, using matched components during module construction.²⁶

Once a circuit is constructed, the next technique is calibration with respect to parameters that can be adjusted, either with hardware or software. This might include gain, phase, and/or group delay. Such calibration might suffice with global values, or may be frequency dependent.

If the characteristic of imbalance holds over temperature, age, etc., then a single calibration will be adequate. However, if imbalance is not static, then repeated or iterative calibration might be required.

In some cases, calibration needs to be adaptive to each and every data set. Examples of such adaptive algorithms include Adaptive Beamforming techniques and Space-Time Adaptive Processing (STAP) for GMTI systems. However, these is not always possible for achieving sufficient balance, and should not substitute entirely for more hardware-centric techniques.

Sometimes channel balance is dependent on signal dynamic range, so can be affected by proper channel gain settings.

2. Move Imbalance Energy

If imbalance cannot be eliminated, sometimes the imbalance energy can be separated from the balanced energy, and then filtered. For example, this can be achieved with channel commutation.^{27,28}

3. Smear Imbalance Energy

Some aspects of imbalance might allow for imbalance energy to be smeared, or otherwise have its coherence suppressed to below the noise level in the data. One example of this might be random phase coding for each channel to decorrelate or decohere spurious signals or cross-talk.

4. Mitigate Effects

Our last line of defense is to mitigate the effects of channel imbalance in a downstream radar product, often after detection operations. Such techniques are often generically referred to as False Alarm Mitigation (FAM) techniques. Specifically, these might include channel averaging, or detection voting schemes.^{29,30}

Otherwise, data-driven autofocus operations can sometimes be employed to alter the transfer functions. Care should be taken to note that such data-driven techniques may exhibit convergence issues that are common to such algorithms.

"The major difference between a thing that might go wrong and a thing that cannot possibly go wrong is that when a thing that cannot possibly go wrong goes wrong it usually turns out to be impossible to get at or repair."

-- Douglas Adams

5 Conclusions

We offer the following summary observations.

- In practice, frequently of greater concern than sibling receiver channels being ideal, is that channels exhibit like characteristics.
- Channel balance is of great concern to a number of radar applications, where we wish to remove the radar hardware/software influence on the relative measurements of various data streams.
- An excellent measure of channel balance between two channels is a measure of the ratio of their transfer functions.
- The ratio measure is related to (but not identical to) a coherence measure between the channels.
- In addition to gain, phase, and delay, channels should ideally exhibit the same noise floor and any nonlinear characteristics, as well as exhibit minimal crosstalk.

"Nothing so needs reforming as other people's habits."
-- Mark Twain

References

.

- ¹ Armin W. Doerry, *Catalog of Window Taper Functions for Sidelobe Control*, Sandia National Laboratories Report SAND2017-4042, Unlimited Release, April 2017.
- ² Armin W. Doerry, *Anatomy of a SAR Impulse Response*, Sandia National Laboratories Report SAND2007-5042, Unlimited Release, August 2007.
- Douglas L. Bickel, SAR Image Effects on Coherence and Coherence Estimation, Sandia National Laboratories Report SAND2014-0369, Unlimited Release, January 2014.
- D. L. Bickel, A. W. Doerry, "Using coherence as a quality measure for complex radar image compression," SPIE 2017 Defense & Security Symposium, Radar Sensor Technology XXI, Vol. 10188, Anaheim, CA, 9-13 April 2017.
- Armin W. Doerry, *Noise and Noise Figure for Radar Receivers*, Sandia National Laboratories Report SAND2016-9649, Unlimited Release, October 2016.
- Armin W. Doerry, Dale F. Dubbert, Bert L. Tise, Effects of Analog-to-Digital Converter Nonlinearities on Radar Range-Doppler Maps, Sandia National Laboratories Report SAND2014-15909, Unlimited Release, July 2014.
- Armin W. Doerry, Dale F. Dubbert, Bert L. Tise, "Spurious effects of analog-to-digital conversion nonlinearities on radar range-Doppler maps," SPIE 2015 Defense & Security Symposium, Radar Sensor Technology XIX, Vol. 9461, Baltimore, MD, 20-24 April 2015.
- A. W. Doerry, D. L. Bickel, A. M. Raynal, "Some comments on performance requirements for DMTI radar," SPIE 2014 Defense & Security Symposium, Radar Sensor Technology XVIII, Vol. 9077, Baltimore MD, 5–9 May 2014.
- Samuel M. Sherman, David K. Barton, Monopulse Principles and Techniques 2nd Edition, ISBN-13: 978-1-60807-174-6, Artech House, Inc., 2011.
- D. L. Bickel, Precomparator and Postcomparator Errors in Monopulse, Sandia National Laboratories Report SAND2013-1287, Unlimited Release, February 2013.
- ¹¹ C. Gierull, *Digital channel balancing of along-track interferometric SAR data*, DRDC Ottawa, Technical Memorandum DRDC-OTTAWA-TM-2003-024, March 2003.
- D. L. Bickel, W. H. Hensley, Design, Theory, and Applications of Interferometric Synthetic Aperture Radar for Topographic Mapping, Sandia National Laboratories Report SAND96-1092, Unlimited Release, May 1996.
- B. Bräutigam, J. Gonzalez, M. Schwerdt, M. Bachmann, "TerraSAR-X instrument calibration results and extension for TanDEM-X," *IEEE Transactions on Geoscience and Remote Sensing*, vol. 48, no. 2, pp. 702–715, February 2010.
- G. Krieger, A. Moreira, H. Fiedler, I. Hajnsek, M. Werner, M. Younis, and M. Zink, "TanDEM-X: A satellite formation for high resolution SAR interferometry," *IEEE Transactions on Geoscience and Remote Sensing*, vol. 45, no. 11, pp. 3317–3341, November 2007.
- J. R. Guerci, Space-Time Adaptive Processing for Radar, ISBN-10: 1580533779, Artech House Radar Library, Artech House, Inc., 2003.
- Taoli Yang, Zhenfang Li, Yanyang Liu, Zheng Bao, "Channel error estimation methods for multichannel SAR systems in azimuth," *IEEE Geoscience and Remote Sensing Letters*, vol. 10, no. 3, May 2013.
- G. Farquharson, P. López-Dekker, and S. J. Fraiser, "Contrast-based phase calibration for remote sensing systems with digital beamforming antennas," *IEEE Transactions on Geoscience and Remote Sensing*, vol. 51, pp. 1744–1754, March 2013.

- Marwan Younis, Christopher Laux, Noora Al-Kahachi, Paco López-Dekker, Gerhard Krieger, and Alberto Moreira, "Calibration of Multi-Channel Spaceborne SAR Challenges and Strategies –," *Proceedings of 10th European Conference on Synthetic Aperture Radar*, EUSAR 2014, Berlin, Germany, 3-5 June 2014.
- M. Younis, T. Rommel, F. de Almeida, S. Huber, M. Martone, M. Villano, G. Krieger, "Investigations on the Internal Calibration of Multi-Channel SAR," *Proceedings of the 2017 IEEE International Geoscience and Remote Sensing Symposium (IGARSS 2017)*, Fort Worth, Texas, USA, 23-28 July 2017.
- J. J. Van Zyl, "Calibration of polarimetric radar images using only image parameters and trihedral corner reflector responses", IEEE Transactions on Geoscience and Remote Sensing, May 1990.
- J. D. Klein, "Calibration of complex polarimetric SAR imagery using backscatter correlations", IEEE Transactions on Aerospace and Electronic Systems, January 1992.
- ²² Anthony Freeman, "SAR Calibration: An Overview," *IEEE Transactions on Geoscience and Remote Sensing*, Vol. 30, No. 6, pp. 1107-1121, November 1992.
- ²³ Armin W. Doerry, *Mitigating I/Q Imbalance in Range-Doppler Images*, Sandia National Laboratories Report SAND2014-2252, Unlimited Release, March 2014.
- Armin W. Doerry, "Balancing I/Q data in radar range-Doppler images," SPIE 2015 Defense & Security Symposium, Radar Sensor Technology XIX, Vol. 9461, Baltimore, MD, 20-24 April 2015.
- A. W. Doerry, "Some comments on GMTI false alarm rate," SPIE 2011 Defense & Security Symposium, Radar Sensor Technology XV, Vol. 8021, pp 80211P, Orlando FL, 25-29 April 2011.
- Peter A. Dudley, Design Guidelines for SAR Digital Receiver/Exciter Boards, Sandia National Laboratories Report SAND2009-7276, Unlimited Release, August 2009.
- ²⁷ Armin W. Doerry, *Radar Channel Balancing with Commutation*, Sandia National Laboratories Report SAND2014-1071, Unlimited Release, February 2014.
- Armin W. Doerry, "Balancing radar receiver channels with commutation," SPIE 2015 Defense & Security Symposium, Radar Sensor Technology XIX, Vol. 9461, Baltimore, MD, 20-24 April 2015.
- Armin W. Doerry, Douglas L. Bickel, *Apodization of Spurs in Radar Receivers Using Multi-Channel Processing*, Sandia National Laboratories Report SAND2014-1678, Unlimited Release, March 2014.
- A. W. Doerry, D. L. Bickel, "Discriminating spurious signals in radar data using multiple channels," SPIE 2017 Defense & Security Symposium, Radar Sensor Technology XXI, Vol. 10188, Anaheim, CA, 9-13 April 2017.

"You can get help from teachers, but you are going to have to learn a lot by yourself, sitting alone in a room." -- Dr. Seuss

Distribution

Unlimited Release

1 1 1	MS 0519 MS 0519 MS 0519	M. R. Lewis A. W. Doerry L. Klein	5349 5349 5349	
1	MS 0532	S. P. Castillo	5340	
1	MS 0899	Technical Library	9536	(electronic copy)

